NLRP3 inflammasome inactivation driven by miR-223-3p reduces tumor growth and increases anticancer immunity in breast cancer

LIPING ZHANG[1], HONGZHI LI[2], YUWEI ZANG[3] and FENG WANG[4]

Departments of [1]Breast Disease and [2]Emergency Surgery, Linyi Central Hospital, Linyi, Shandong 276499; [3]Department of Radiology, Yishui People's Hospital, Linyi, Shandong 276428; [4]Department of Breast Disease, Beijing Tiantan Hospital, Capital Medical University, Beijing 100050, P.R. China

Received March 26, 2018; Accepted November 7, 2018

DOI: 10.3892/mmr.2019.9889

Abstract. MicroRNA-233-3p (miR-223-3p) is considered an important cancer-associated marker. The NACHT, LRR and PYD domains-containing protein 3 (NLRP3) inflammasome represents a novel potential target for the treatment of breast cancer. Therefore, it was hypothesized that miR-223-3p may affect tumor growth and immunosuppression in breast cancer by inhibiting the NLRP3 inflammasome. In the present study, an increased expression level of NLRP3 was detected in three breast cancer cell lines compared with normal mammary epithelial cells (HMEC). Suppressing the expression of NLRP3 in MCF-7 cell lines increased the apoptotic rate of breast cancer cells and reduced the proliferative capacity. NLRP3 was identified to be a direct target of miR-233-3p using a luciferase assay. In addition, miR-233-3p mimics inhibited the NLRP3-dependent processes in cancer cells by suppressing the NLRP3 expression level and the protein expression levels of its downstream factors, including PYD and CARD domain containing protein, interleukin-1β and interleukin-18. *In vivo* experiments demonstrated the suppressive effect of miR-233-3p in tumor growth and immunosuppression. Collectively these findings suggested that the inactivation of the NLRP3 inflammasome driven by miR-223-3p reduced the growth and immunosuppression of breast cancer *in vitro* and *in vivo,* and may represent a novel therapeutic strategy in treating breast cancer.

Introduction

Breast cancer is one of the most common types of cancer, accounting for 7-10% of systemic malignancies, and is a serious health threat to women worldwide (1). Surgery and chemotherapy may decrease the risk of local recurrence or non-localized breast cancer (2). However, local and regional treatment outcomes remain unsatisfactory due to the lack of specific molecular markers and therapeutic targets (3). Therefore, understanding the molecular mechanisms of breast cancer may improve diagnoses and clinical outcomes.

Inflammasomes are multiprotein complexes regulating various inflammatory factors, including interleukin-1β (IL-1β) and interleukin-18 (IL-18). IL-18 induces programmed cell death protein 1-dependent immunosuppression in cancer (4), and IL-1β is one of the most important inflammatory mediators eliciting immunosuppressive properties (5). Therefore, these cytokines serve important roles in tumorigenesis. NACHT, LRR and PYD domains-containing protein 3 (NLRP3) is the most widely studied inflammasome. A previous study demonstrated that activated NLRP3 significantly promoted the protein expression level of IL-18 in the plasma of patients with lymphoma (6). Furthermore, it was identified that the activation of caspase-1 may trigger the maturation and secretion of IL-18 (7). Additionally, a previous study observed that the NLRP3 inflammasome components were upregulated in biopsies from head and neck squamous cell carcinoma tissues, suggesting that the NLRP3 inflammasome may serve crucial functions in the survival and invasion of human head and neck squamous cell carcinoma (8). However, the role of NLRP3 inflammasome activation in breast cancer and its underlying mechanism of action remain unclear.

MicroRNAs (miRNAs) regulate a variety of important biological processes in cells, including cell proliferation, differentiation and invasion (9). Furthermore, dysregulation of miRNAs may contribute to cancer formation (10). miRNA-107 was associated with breast cancer progression and negatively regulated the expression of cyclin dependent kinase 8 inhibiting the proliferation of breast cancer cells *in vitro* (11). Additionally, a previous study demonstrated that miRNA-223-3p (miR-233) was involved in embryo implantation by suppressing pinopode formation and leukemia inhibitory factor protein expression (12). Furthermore, miR-233 downregulated the nuclear factor κ-light-chain-enhancer of activated B cells signaling to attenuate neutrophilic inflammation (13). These previous studies suggested that miR-233 may balance the inflammatory response.

Correspondence to: Professor Feng Wang, Department of Breast Disease, Beijing Tiantan Hospital, Capital Medical University, 119 South Fourth Ring Road, Beijing 100050, P.R. China
E-mail: fengwangly@sina.com

Key words: breast cancer, inflammasome, microRNA-223-3p, NACHT, LRR and PYD domains-containing protein 3

The present study suggested that miR-233 suppressed the growth of breast cancer cells via a mechanism associated with the inactivation of the NLRP3 inflammasome. The present results provided novel insight into the molecular functions of miR-233 in regulating the NLRP3 inflammasome in breast cancer cells.

Materials and methods

Cell culture and RNA transfection. HMEC, MDA-MB231, MCF-7 and SKBR3 cell lines were purchased from the Type Culture Collection of The Chinese Academy of Sciences (Bena Culture Collection, Shanghai, China). MDA-MB231 and SKBR3 cell lines were maintained in RPMI-1640 medium (Sigma-Aldrich; Merck KGaA, Darmstadt, Germany) containing 10% fetal bovine serum (FBS; Gibco; Thermo Fisher Scientific, Inc., Waltham, MA, USA) with 100 mg/ml streptomycin and 100 U/ml penicillin. MCF-7 cell lines and HMEC cells were cultured in Dulbecco's modified Eagle's medium (Thermo Fisher Scientific, Inc.) containing 10% FBS, 100 mg/ml streptomycin and 100 U/ml penicillin. Cells were passaged with PBS (Sigma-Aldrich; Merck KGaA) and 0.02% EDTA/0.5% trypsin (GE Healthcare, Chicago, IL, USA) every 3 days. All cells were cultured with 5% CO_2 at 37˚C until further experiments were performed.

The short hairpin (sh)-NLRP3, miRNA mimics, inhibitors and the scrambled negative control oligonucleotides were purchased from Guangzhou RiboBio Co., Ltd. (Guangzhou, China) and 1,000 ng/μl used for the transfection of MCF-7 cells with Lipofectamine® 2000 (Invitrogen; Thermo Fisher Scientific, Inc.). Transfection was performed with Lipofectamine® 2000 (Invitrogen; Thermo Fisher Scientific, Inc.) according to the manufacturer's protocol. In total, $2x10^4$ cells/well were seeded into six wells and each sample was transfected with 0.2 mg RNA. Following transfection, cells were incubated at 37˚C with 5% CO_2 for 24 or 48 h.

Reverse transcription-quantitative polymerase chain reaction (RT-qPCR). miRNA was extracted from cells using the miRNeasy FFPE kit (Qiagen China Co., Ltd., Shanghai, China). Primers for miR-233 (cat. no. HmiRQP0339; ATA TAGCATCTTTCTGTCTCGCCCATCCCGTTGCTCCAA TATTCTAACAACAAGTGATTATTGAGCAATGCGCAT GTGCGGGATAGACTGATGGCTGC) were obtained from GeneCopoeia, Inc. (Rockville, MD, USA). NLRP3 primers were forward, 5'-AGACCTCCAAGACCACTAC-3' and reverse, 5'-ACATAGCAGCGAAGAACTC-3'. Total RNA was extracted from the cells using RNeasy Mini kit (Qiagen, Hilden, Germany) according to the manufacturer's protocol. The extracted RNA was reverse transcribed into cDNA using the ThermoScript™ RT-PCR system at 40˚C for 2 h (Invitrogen; Thermo Fisher Scientific, Inc.). RT-qPCR was performed using the 7500 Real-Time PCR system (Applied Biosystems; Thermo Fisher Scientific, Inc.) using appropriate primers and the fluorescent dye SYBR Green (Takara Biotechnology Co., Ltd., Dalian, China). For quantification of mature miRNA, cDNA was generated using specific stem-loop universal primers. PCR reaction mixtures were set up in a total volume of 20 μl. Standard PCR settings (95˚C for 30 sec, 40 cycles of 95˚C for 5 sec and 60˚C for 34 sec, followed by a dissociation stage for 15 sec at 95˚C, 1 min at 60˚C and 15 sec at 95˚C) were used. All samples were run in duplicates. GAPDH was selected as the normalization control gene. The same RT-qPCR protocol was used for all the genes and miRNA analyzed. Results are expressed as fold change with respect to the experimental control. Quantitation was according to $R=(1+E1)^{\Delta Ct1}$ (Control-Sample)/$(1+E2)^{\Delta Ct2}$ (Control-Sample) method (14).

Western blot analysis. Cells and tissues were homogenized in radioimmunoprecipitation assay buffer (Thermo Fisher Scientific, Inc.). The protein concentration was determined using a Bicinchoninic Acid protein assay kit (Thermo Fisher Scientific, Inc.), and 50 μg protein was loaded per lane with 5% concentrated SDS gels and 15% separating gel. Following electrophoresis, the gel was transferred onto a 0.45 μm polyvinylidene fluoride membrane (Merck KGaA). Following transfer, the membranes were blocked for 2 h with 5% nonfat dry milk at room tempreture. Subsequently, the membranes were incubated overnight at 4˚C with anti-NLRP3 (15101; 1:500), anti-proliferation marker protein Ki67 (9129; 1:1,000; Ki67; both CST Biological Reagents Co., Ltd., Shanghai, China), anti-vascular endothelial growth factor (VEGF; ab32152; 1:500 Abcam, Cambridge, UK), anti-PYD and CARD domain-containing protein (ASC; sc-271054; 1:500; Santa Cruz Biotechnology, Inc., Dallas, TX, USA), anti-IL-1β (ab200478; 1:500), anti-IL-18 (ab71495; 1:500; both Abcam) and anti-GAPDH (35174.; 1:1,000) primary antibodies, followed by incubation with secondary antibody conjugated to horseradish peroxidase (7074; 1:1,000; both CST Biological Reagents Co., Ltd.) at room tempreture for 2 h. Following washing with TBS, proteins were visualized using enhanced chemiluminescence reagents Rabbit IgG (Pierce; Thermo Fisher Scientific, Inc.), according to the manufacturer's protocol. ImageJ (version number: 1.4.3.67; National Institutes of Health, Bethesda, MD, USA) was used for densiometric analysis.

Hoechst staining. Coverslips were soaked in 70% ethanol for 5 min, the cells were washed three times with 0.9% NaCl and the coverslips were placed in 6-well plates and incubated at 37˚C with 5% CO_2 overnight. Cells were stimulated to undergo apoptosis by 100 μM H_2O_2 for 1 h. Subsequently, the culture solution was discarded and 0.5 ml 4% paraformaldehyde fixative solution was added for 10 min at 37˚C. The fixative was removed and cells were washed twice with 0.9% NaCl for 3 min, and the washing solution was discarded. A total of 0.5 ml Hoechst 33258 staining solution was added and cells were stained for 5 min at 37˚C. The slides were sealed with antifluorescence quenching sealant, and imaged using fluorescence microscopy for 20 fields of view and the analysis were used for Image J version 1.8.0 (National Institutes of Health).

Transwell assay. To analyze cell migration, $2x10^5$ cells were seeded in six-well plates in triplicate. A Transwell chamber was placed into the culture plate, with the upper chamber containing the upper culture medium (DMEM) and the lower chamber containing the lower culture medium (DMEM). The upper and lower culture media were separated by a polycarbonate membrane. Following 7 days, cells were plated in the

upper chamber and the growth and migration of cells in the lower culture medium. The cells were stained with 0.1% crystal violet for 20 min at room temperature and the unmigrated cells in the upper layer were gently wiped off with a cotton swab and washed 3 times with PBS and using a light microscope with magnification, x10. All experiments were performed in triplicates and error bars indicate the standard deviation.

Cell proliferation assay. A cell proliferation assay was performed using a Cell Counting kit-8 (CCK-8). A total of $2x10^5$ cells were plated into 96-well culture plates. Following 24 h incubation, CCK-8 solution was added to each well and incubated for 4 h (1 mg/ml; Sigma-Aldrich; Merck KGaA) at 37˚C with 5% CO_2. The absorbance was measured at 450 nm. Each experiment was performed at least three times, each with triplicate samples.

Luciferase reporter assay. Association between miR-223 and NLRP3 was predicted using the online software Targetscan (http://www.targetscan.org/vert_71). NLRP3 3' untranslated region (3'UTR) wild-type (WT) 5'-CGCUAUCUUUCU AUUAACUGACC-3', was cloned downstream of the *Renilla* luciferase gene (pLUC-REPORT vector; Promega Corporation, Madison, WI, USA). A pLUC-REPORT construct containing a mutant (Mut) NLRP3 3'UTR sequence corresponding to the miR-233-3p binding site was generated using the following sequence: 5'-CGCUAUCUUUCUAUUUUCUCUCC-3'. For the luciferase reporter assay, MCF-7 cells were cotransfected using Lipofectamine® 2000 (Thermo Fisher Scientific, Inc.) with a luciferase reporter vector containing the WT or Mut version of NLRP3 and the miR-233-3p mimics plasmid and the pEZX-MR04 plasmid containing miR-233-3p precursor construct or its scrambled control equivalent pEZX-MR04 with 2.5 μg/μl (GeneCopoeia, Inc.). Luciferase activity was measured at 48 h following transfection using a dual-luciferase assay kit (Promega Corporation) and normalized to firefly luciferase activity. A total of three independent experiments were performed in triplicate.

Ethics approval. The animal experiments in the present study were approved by The Animal Care and Research Committee of Beijing Tiantan Hospital (Beijing, China). All experiments were performed in compliance with relevant laws and guidelines. All experiments were conducted following the institutional guidelines of Beijing Tiantan Hospital.

Tumor volume and survival curve. The total of 100 female mice were purchased from The Institute of Zoology, Chinese Academy of Medical Sciences (Bejing, China). The animals were 8 weeks old and 20-22 g in weight. The mice were kept in clean rooms at a temperature of ~25˚C with a humidity of 75%, 12-h light/dark cycle and food and water *ad libitum*. A total of $3x10^6$ MCF-7 cells transfected with miR-223 mimics were injected subcutaneously into the shoulder scapula (n=5) of the nude mice and the tumor volume was assessed by the formula: Tumor volume (mm^3) = maximal length (mm) x perpendicular width $(mm)^2/2$ every 5 days. All mice were sacrificed following measurements. The number of surviving nude mice was measured and survival curves were calculated.

Immunohistochemistry. Sections of 5 μm in thickness were prepared using tissue blocks embedded in paraffin and fixed using 4% formaldehyde overnight at room tempreture, followed by deparaffinization and hydration using xylene and graded alcohol series. The sections were treated with a sodium citrate buffer in a microwave for antigen retrieval and blocked using normal goat serum. Then washed 3 times with PBS for 5 min each time. Subsequently, sections were stained using rabbit anti-terminal deoxynucleotidyl transferase (1:100), anti-Ki67 (1:100) or anti-VEGF (1:100; all Abcam) overnight at 4˚C, and subsequently incubated with a biotinylated goat anti-rabbit immunoglobulin G secondary antibody for 1 h, followed by staining with an avidin-biotin peroxidase complex (GeneTex, Inc., Irvine, CA, USA).

ELISA. Blood samples were collected by enucleation. Subsequently, samples were kept at room temperature for 2 h and centrifuged at 2,000 x g for 30 min with 25˚C. Subsequently, serum was transferred into 1.5 ml polypropylene tubes, and stored at -20˚C. Protein expression levels of IL-1β, IL-18 and IL-10 in the serum were determined using an ELISA kit (Yinggong Corporation, Shanghai, China) according to the manufacturer's protocol, at 450 nm.

Statistical analysis. SPSS (version 22.0; IBM Corp., Armonk, NY, USA) software was used for statistical analysis. Data obtained from experiments using cultured cells are presented as the mean ± standard deviation. Statistical analysis of normal distribution was performed on two independent samples. Differential expression of miRNAs was detected by t-test or one-way analysis of variance (ANOVA). Survival curves were analyzed using Kaplan-Meier method and log-rank test. One-way analysis of variance was followed by a post hoc test for difference value calculation, and Mann-Whitney U tests were performed to determine statistical differences in viability between miR-233- and scramble-transfected cells in case of non-normal distributions. Qualitative data were representative of more than three independent experiments, with each performed in triplicate. $P<0.05$ was considered to indicate a statistically significant difference.

Results

Transfection of sh-NLRP3 affects the expression of NLRP3 in MCF-7 cells. NLRP3 expression levels were measured in three breast cancer cell lines (MDA-MB231, MCF-7 and SKBR3) and normal mammary epithelial cells (HMEC). An increase in the NLRP3 expression level was observed in the breast cancer cells compared with HMEC (Fig. 1A). Among the three cancer cell lines, the highest expression level of NLRP3 was measured in MCF-7 cells. Subsequently, the effect of sh-NLRP3 on MCF-7 cells was investigated. Transfection with sh-NLRP3 decreased the NLRP3 expression level in MCF-7 cell lines, suggesting that transfection with sh-NLRP3 affected the expression of NLRP3 in MCF-7 cell lines (Fig. 1B and C).

sh-NLRP3 inhibits human breast cancer MCF-7 cell growth and migration in vitro. Subsequently, the effects of sh-NLRP3 on cell function were investigated in breast cancer cells. The

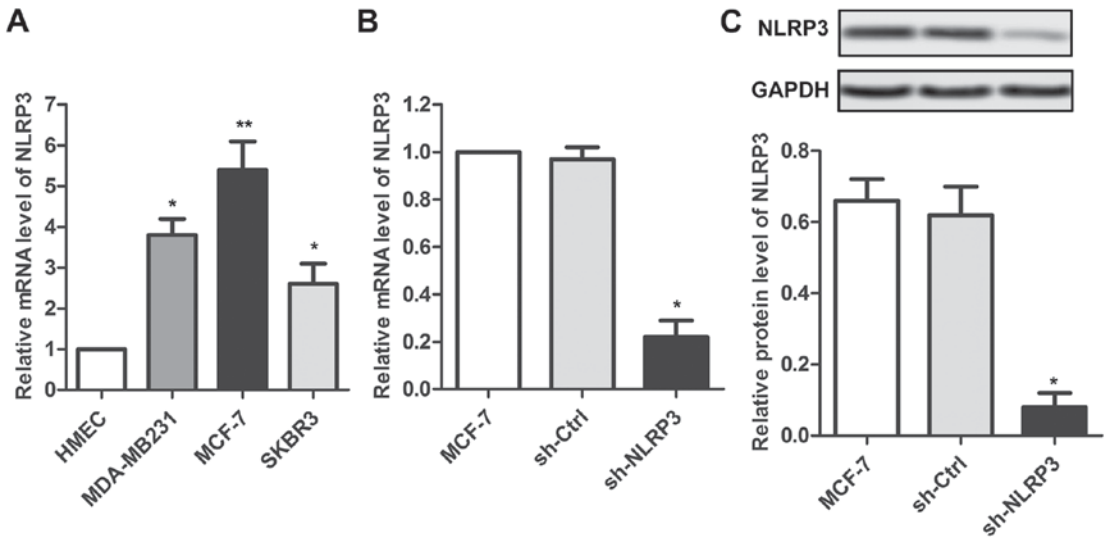

Figure 1. sh-NLRP3 suppresses the expression of NLRP3 in MCF-7 cells. (A) NLRP3 expression was detected in three breast cancer cell lines (MDA-MB231, MCF-7 and SKBR3) and in HMECs by RT-qPCR. *P<0.05, **P<0.01 vs. HMEC. (B) sh-NLRP3 was transfected into MCF-7 cells. NLRP3 expression was detected 48 h following transfection by RT-qPCR. An empty plasmid was used as the negative control. (C) NLRP3 expression was detected by western blot analysis using anti-NLRP3 48 h following transfection. *P<0.05 vs. MCF-7. RT-qPCR, reverse transcription-quantitative polymerase chain reaction; sh, short hairpin; NLRP3, NACHT, LRR and PYD domains-containing protein 3; Ctrl, control.

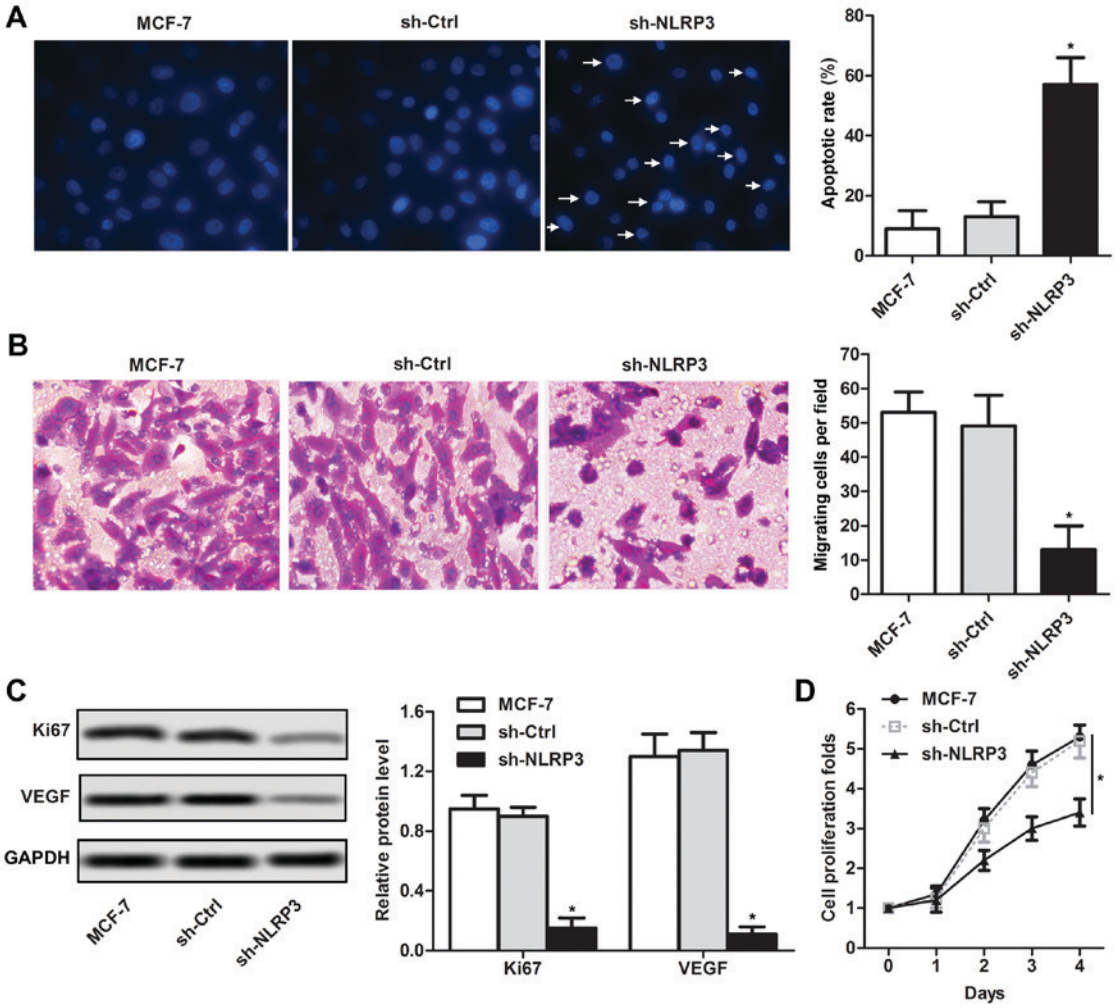

Figure 2. sh-NLRP3 inhibits the growth and migration of human breast cancer cells MCF-7 *in vitro*. (A) Percentage of apoptotic cells in three groups was detected by performing Hoechst staining. White arrows, nucleus (magnification, x400). (B) Cell migration measured by Transwell analysis (magnification, x400). (C) Protein expression levels of Ki67 and VEGF were detected by western blotting. (D) Proliferation of breast cancer cells following treatment with sh-NLRP3 and with sh-Ctrl was measured by Cell Counting kit-8. *P<0.05 vs. respective MCF-7. NLRP3, NACHT, LRR and PYD domains-containing protein 3; sh, short hairpin; VEGF, vascular endothelial growth factor; Ctrl, control; Ki67, proliferation marker protein Ki67.

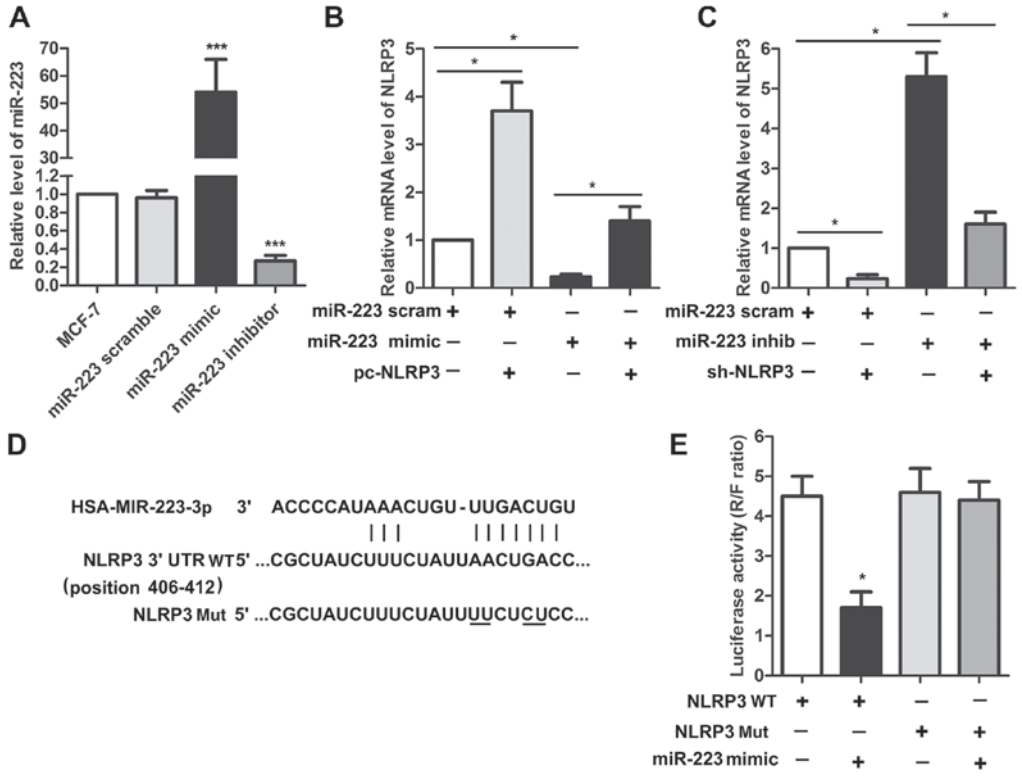

Figure 3. miR-223 and NLRP3 are inversely associated in human breast cancer cells. (A) Expression of miR-223 was measured by RT-qPCR. ***P<0.001 vs. MCF-7. (B) Effect of miR-223 mimics alone and in combination with pcDNA-NLRP3 on NLRP3 expression was measured by RT-qPCR. (C) Effect of miR-223 inhibitor alone and in combination with sh-NLRP3 on NLRP3 expression was detected by RT-qPCR. *P<0.05. (D) Association between miR-223 and NLRP3 was predicted using the online software Targetscan (http://www.targetscan.org/vert_71). (E) Effect of miR-223 mimics on NLRP3 WT and NLRP3 Mut was detected by a luciferase assay. *P<0.05 vs. NLRP3 WT. miR, microRNA; NLRP3, NACHT, LRR and PYD domains-containing protein 3; RT-qPCR, reverse transcription-quantitative polymerase chain reaction; sh, short hairpin; WT, wild-type; Mut, mutant; 3'UTR, 3' untranslated region; scram, scramble; inhib, inhibitor.

percentage of apoptotic cells following sh-NLRP3 transfection was significantly higher compared with the MCF-7 control group (Fig. 2A). The Transwell analysis suggested that the migratory ability following sh-NLRP3 transfection was significantly lower compared with the MCF-7 control group (Fig. 2B). Decreased protein expression levels of Ki67 and VEGF were detected in the sh-NLRP3 group compared with the MCF-7 control group, by western blotting (Fig. 2C). To further investigate whether cell proliferation was affected following transfection with sh-NLRP3, a CCK-8 assay was conducted. sh-NLRP3 transfection significantly decreased the cell proliferation rate in MCF-7 cell lines at 4 days (Fig. 2D). The present data suggested that sh-NLRP3 inhibited the growth and migration of MCF-7 cells *in vitro*.

miR-233 and NLRP3 are inversely correlated in human breast cancer cells. The physical association between miR-223 and NLRP3 was predicted by online software Targetscan. The expression of miR-223 was detected using RT-qPCR in MCF-7 cells transfected with miR-223 mimics or miR-223 inhibitor. The present results demonstrated that miR-223 was significantly increased in the miR-223 mimics group and was significantly decreased following miR-223 inhibitor transfection compared with the MCF-7 control (Fig. 3A). Subsequently, the effect of miR-223 mimics alone or in combination with pcDNA-NLRP3 on the expression level of NLRP3 was examined. The present results suggested that the upregulation of NLRP3 following NLRP3 overexpression was attenuated by cotransfecting miR-223 mimics (Fig. 3B). Furthermore, the upregulation of NLRP3 following miR-223 inhibitor transfection was inhibited by sh-NLRP3 (Fig. 3C). The present results suggested that miR-223 and NLRP3 are inversely associated in human breast cancer cells. Additionally, the effects of miR-223 mimics on the luciferase activity of a reporter plasmid containing NLRP3 WT 3'UTR or NLRP3 Mut 3'UTR were detected by a luciferase assay. The present results suggested that miR-223 mimics decreased the NLRP3 expression level only when cotransfected with NLRP3 WT and not with NLRP3 Mut (Fig. 3D and E).

miR-233 suppresses the growth, migration and NLRP3 inflammasome activity in human breast cancer cells by inhibiting the NLRP3 pathway. To further investigate the association between miR-233 and NLRP3 in human breast cancer cells, NLRP3 was overexpressed by transfecting cells with a pcDNA vector containing NLRP3. The present results suggested that NLRP3 promoteed the growth of breast cancer cells, while miR-233 could inhibit its proliferation at the tissue level (Fig. 4A). Similarly, at the protein level, overexpression of NLRP3 and miR-233 scrambled upregulated the expression of Ki67 and VEGF, indicating the downregulation of NLRP3 by miR-233 (Fig. 4B). NLRP3 overexpression attenuated the inhibitory effect of miR-223 mimics on cell growth (Fig. 4A-C). Subsequently, the protein expression levels of ASC, IL-1β and IL-18 were investigated. The present results suggested that the increased ASC, IL-1β and IL-18

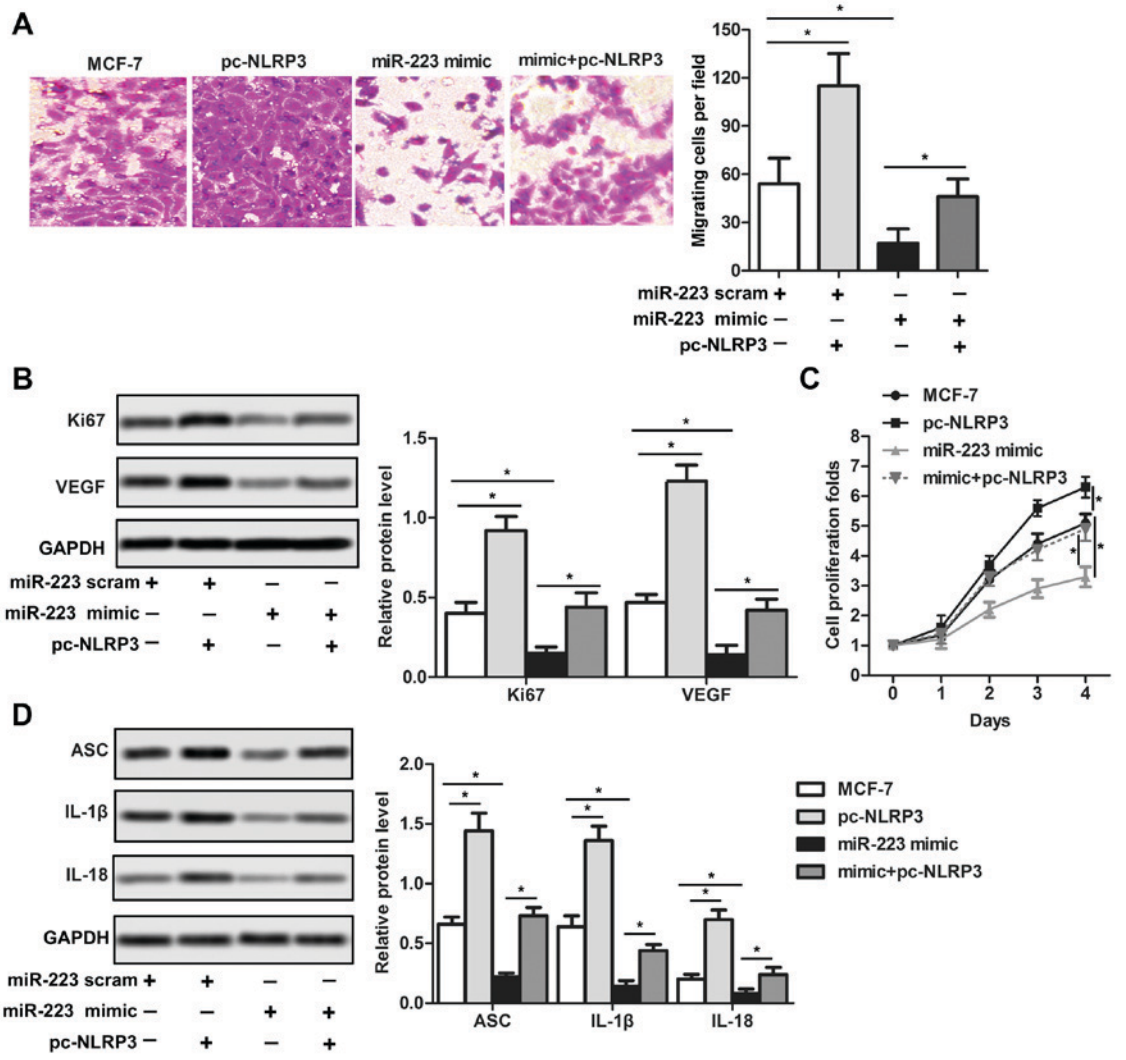

Figure 4. miR-233 suppresses the growth and migration of human breast cancer cells by inactivating the NLRP3 pathway. (A) Cell migration was measured by Transwell assays (magnification, x400). (B) Ki67 and VEGF protein expression levels were detected by western blotting. (C) Cell proliferation of breast cancer cells following transfection with miR-223 mimics and pc-NLRP3 was measured by Cell Counting kit-8. (D) Protein expression levels of ASC, IL-1β and IL-18 were detected by western blotting. *P<0.05. miR, microRNA; NLRP3, NACHT, LRR and PYD domains-containing protein 3; IL-, interleukin; ASC, PYD and CARD domain-containing protein; VEGF, vascular endothelial growth factor; Ki67, proliferation marker protein Ki67; scram, scramble.

protein expression levels induced by NLRP3 overexpression were decreased by miR-223 mimics (Fig. 4D).

NLRP3 inflammasome inactivation by miR-233 decreases the tumor volume in vivo. To investigate the inhibitory effects of miR-233 on tumor progression, MCF-7 cells transfected with miR-223 mimics were subcutaneously injected into nude mice. The results suggested that the tumor volume was significantly lower in the miR-223 mimics group compared with the MCF-7 control group following 20 and 25 days (Fig. 5A). Furthermore, the survival rate was increased in the miR-223 mimics group compared with the negative control groups (Fig. 5B). Subsequently, the number of cells expressing Ki67 and/or VEGF was analyzed by immunohistochemistry. An increased apoptotic rate and decreased number of Ki67- and VEGF-positive cells were detected in the miR-223 mimics group compared with the negative control group (Fig. 5C). Additionally, the downstream pathway of NLRP3 was investigated. The results demonstrated that miR-223 overexpression led to a decrease in the protein expression levels of ASC, and the concentration of serum IL-1β and IL-18 decreased; however, the IL-10 protein expression level increased (Fig. 5D and E). The association between NLRP3 and miR-223 in breast cancer is depicted in Fig. 6. Collectively, the present data suggested that miR-233 reduced growth and immunosuppression of breast cancer via inactivation of the NLRP3 inflammasome *in vivo*.

Discussion

Activation of the NLRP3 inflammasome has a critical role in disease development (15-18). NLRP3 activation was implicated in a number of pathophysiological processes, including chronic liver disease, lymphoma and cancer (19,20). Consistent with previous studies (21), the present results suggested that NLRP3 expression was higher in the three breast cancer cell lines tested, compared with HMEC cells. Considering the increased expression level of NLRP3 in MCF-7 cells compared with the other two cell lines (MDA-MB231 and SKBR3), it was hypothesized that the knockdown of NLRP3 may be more effective in MCF-7 cells. Therefore, the MCF-7 cell line was

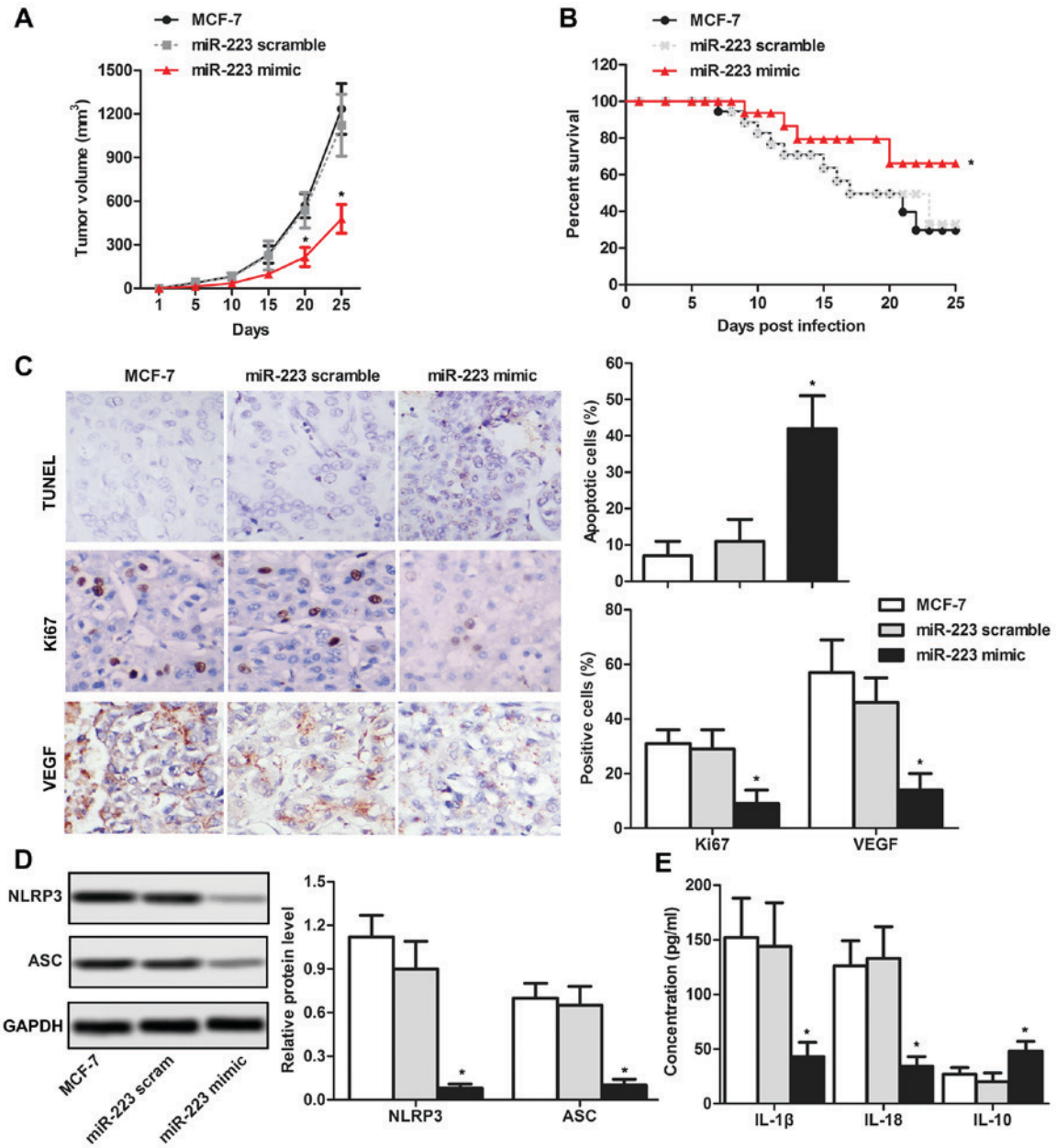

Figure 5. NLRP3 inflammasome inactivation driven by miR-233 reduces the development of tumors *in vivo*. (A) Tumor volume was measured by subcutaneously injecting MCF-7 cells transfected with miR-223 mimics into nude mice. (B) Survival curve of nude mice was measured for 25 days. (C) Expression level of TUNEL, Ki67 and VEGF were detected by immunohistochemistry (magnification, x400). (D) Protein expression levels of NLRP3 and ASC were detected by western blotting. (E) Concentrations of IL-1β, IL-18 and IL-10 were detected by ELISA. *P<0.05 vs. respective MCF-7. NLRP3, NACHT, LRR and PYD domains-containing protein 3; IL-, interleukin; ASC, PYD and CARD domain containing protein; TUNEL, terminal deoxynucleotidyl transferase dUTP nick end labeling; miR, microRNA; Ki67, proliferation marker protein Ki67; scram, scramble.

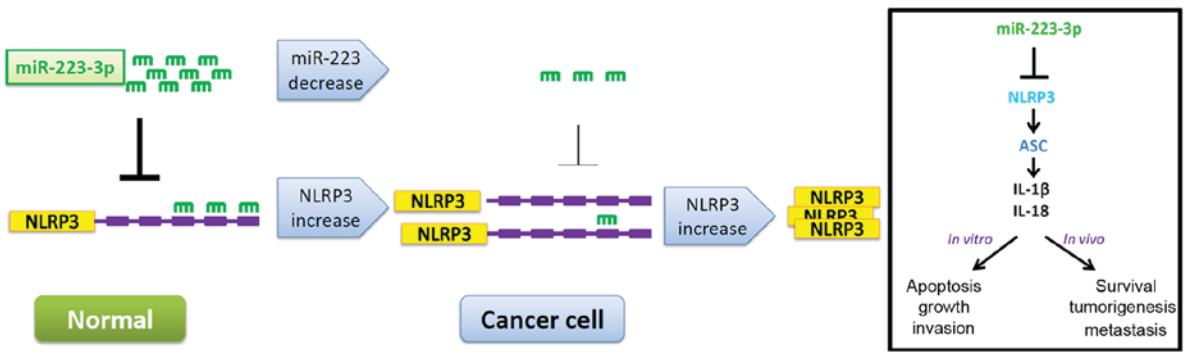

Figure 6. Schematic model of miR-223 regulating cancer growth and immunosuppression by targeting NLRP3 in breast cancer. NLRP3, NACHT, LRR and PYD domains-containing protein 3; miR, microRNA; ASC, PYD and CARD domain containing protein; IL-, interleukin.

used for subsequent *in vitro* and *in vivo* experiments. Following NLRP3 knockdown, decreased proliferation rates and increased apoptotic rates of MCF-7 cells were detected, suggesting that NLRP3 may contribute to the progression of breast cancer. However, the present study presents certain limitations, due to the fact that MDA-MB231, MCF-7 and SKBR3 are three different subtypes of breast cancer cell lines. MCF-7 is estrogen receptor (ER)- and progesterone receptor (PR)-positive (22,23), and SKBR3 is human epidermal growth factor receptor 2 (HER2)-positive, whereas, MDA-MB231 is ER-, PR- and HER2-negative (24,25). Considering the limitations of the present study, further studies are required to investigate the role of the miR223-NLRP3 axis in MDA-MB231 and SKBR3 cells.

According to the present results, NLRP3 knockdown induced cell apoptosis in MCF-7 cells and decreased cell migration. In order to investigate whether the inhibitory effect of shRNA-NLRP3 on the migratory ability was not due to increased apoptosis, the expression level of VEGF, a biomarker of cell migration, was tested. A significant downregulation of VEGF was detected following NLRP3 knockdown, suggesting an inhibitory effect of shRNA-NLRP3 on cell migration. In order to further investigate this phenomenon, the effects of NLRP3 knockdown on epithelial-mesenchymal transition (testing cellular morphology, E-cadherin and N-cadherin) of breast cancer cells require investigation in the future. A previous study demonstrated that miR-233 regulated cell growth and angiogenic properties in cancer cells (26). In the present study, miR-233 reduced proliferation via a mechanism that may be associated with the inactivation of the NLRP3 inflammasome and its downstream proteins ASC, IL-1β and IL-18. Previous studies have suggested that the NLRP3 inflammasome was able to activate caspase-1, which induced the maturation and secretion of IL-1β and IL-18 in cancer (7,27). A previous study demonstrated that secreted IL-10 was associated with the downregulation of nigericin-induced NLRP3 inflammasome activation in cultured and primary human immune cells (28). Additionally, IL-10 and miR-233 were identified as regulators of NLRP3 in *Helicobacter pylori*-infected cells (29). In the present study, the protein expression level of IL-10 was increased following NRLP3 downregulation driven by the miR-223 mimics group. The results were in agreement with previous studies that demonstrated an increased immune response following NLRP3 inhibition (30,31). Additionally, the present study identified a decrease in the expression level of ASC, IL-1β and IL-18 in the miR-223 mimics group. Inflammatory cytokines, ASC, IL-1β and IL-18, are aberrantly expressed in inflammatory-associated diseases and have oncogenic effects in specific types of cancer, including gastric cancer. Deswaerte *et al* (32) suggested a significant positive association between an elevated mature IL-18 protein expression level and ASC mRNA expression levels in cancer. These factors may represent novel therapeutic targets in cancer, and the long-term objective of breast cancer research is to identify novel targets for clinical diagnosis and the treatment of breast cancer. In the present study, the expression level of NLRP3 increased following miR-233 inhibition in MCF-7 cells. The present finding suggested that miR-233 may affect the progression of breast cancer cells by inactivating the NLRP3 inflammasome.

Huang *et al* (33) suggested that miR-223 may increase proliferation, promote invasion, and inhibit apoptosis of lung cancer A549 cells via activation of the nuclear factor κ-light-chain-enhancer of activated B cells signaling pathway. However, Guo *et al* (34) identified that miR-233 inhibited bladder carcinoma invasiveness via nuclear receptor coactivator 1. These previous studies demonstrated the various effect of miR-233 on tumor development. In order to investigate the mechanism of miR-233 function in breast cancer progression, *in vivo* experiments were performed in the present study. The present results suggested that miR-233 inhibited the growth of tumors and increased the survival rate of experimental mice. Overexpression of miR-233 suppressed tumor growth, suggesting an inhibitory role for miR-233 in breast cancer progression. Consistent with the present *in vitro* results, overexpression of miR-233 significantly decreased the expression level of the NLRP3 inflammasome *in vivo*. Although a previous study demonstrated that miR-233 regulated ovarian cancer cell proliferation and invasion by targeting sex-determining region Y-box 11 expression (35), the function of miR-233 and the association between miR-233 and NLRP3 in breast cancer was not examined in previous studies, to the best of the authors' knowledge. These present results suggested that NLRP3 inflammasome inactivation driven by miR-233 reduced the growth of breast cancer *in vivo*.

Collectively, the present study demonstrated that miR-233 may suppress breast cancer cell growth via a mechanism associated with the inactivation of the NLRP3 inflammasome *in vitro* and *in vivo*. The miR-233/NLRP3-mediated cancer pathway was identified as a molecular mechanism regulating the growth and immunosuppression of breast cancer, and may represent a therapeutic target for the treatment of breast cancer.

Acknowledgements

The authors would like to thank Dr Yuwei Zang, Dr Feng Wang and the members of The Linyi Central Hospital (Linyi, China) and Beijing Tiantan Hospital, for providing technical support to the present study.

Funding

The present study was funded by The Youth Foundation of Beijing Tiantan Hospital, Capital Medical University, Beijing, China (grant no. 2015-YQN-09).

Availability of data and materials

The datasets used and/or analyzed during the current study are available from the corresponding author on reasonable request.

Authors' contributions

LZ analyzed and interpreted the principal data regarding the cell transfection and *in vitro* experiments. HL and YZ were involved in the *in vivo* experiments and statistical analysis. FW was responsible for the design of the study and drafting the manuscript. All authors read and approved the final manuscript.

Ethics approval and consent to participate

The animal experiments in the present study were approved by The Animal Care and Research Committee of Beijing Tiantan

Hospital. All experiments were performed in compliance with relevant laws and guidelines. All experiments were conducted following the institutional guidelines of Beijing Tiantan Hospital.

Patient consent for publication

Not applicable.

Competing interests

The authors declare that they have no competing interests.

References

1. Sun Q, Liu T, Yuan Y, Guo Z, Xie G, Du S, Lin X, Xu Z, Liu M, Wang W, *et al*: MiR-200c inhibits autophagy and enhances radiosensitivity in breast cancer cells by targeting UBQLN1. Int J Cancer 136: 1003-1012, 2015.
2. Darby S, McGale P, Correa C, Taylor C, Arriagada R, Clarke M, Cutter D, Davies C, Ewertz M, Godwin J, *et al*: Effect of radiotherapy after breast-conserving surgery on 10-year recurrence and 15-year breast cancer death: Meta-analysis of individual patient data for 10,801 women in 17 randomised trials. Lancet 378: 1707-1716, 2011.
3. Deng L, Lei Q, Wang Y, Wang Z, Xie G, Zhong X, Wang Y, Chen N, Qiu Y, Pu T, *et al*: Downregulation of miR-221-3p and upregulation of its target gene PARP1 are prognostic biomarkers for triple negative breast cancer patients and associated with poor prognosis. Oncotarget 8: 108712-108725, 2017.
4. Terme M, Ullrich E, Aymeric L, Meinhardt K, Desbois M, Delahaye N, Viaud S, Ryffel B, Yagita H, Kaplanski G, *et al*: IL-18 induces PD-1-dependent immunosuppression in cancer. Cancer Res 71: 5393-5399, 2011.
5. Fan H, Zhao G, Liu L, Liu F, Gong W, Liu X, Yang L, Wang J and Hou Y: Pre-treatment with IL-1β enhances the efficacy of MSC transplantation in DSS-induced colitis. Cell Mol Immunol 9: 473-481, 2012.
6. Zhao X, Zhang C, Hua M, Wang R, Zhong C, Yu J, Han F, He N, Zhao Y, Liu G, *et al*: NLRP3 inflammasome activation plays a carcinogenic role through effector cytokine IL-18 in lymphoma. Oncotarget 8: 108571-108583, 2017.
7. Martinon F, Burns K and Tschopp J: The inflammasome: A molecular platform triggering activation of inflammatory caspases and processing of proIL-beta. Mol Cell 10: 417-426, 2002.
8. Bae JY, Lee SW, Shin YH, Lee JH, Jahng JW and Park K: P2X7 receptor and NLRP3 inflammasome activation in head and neck cancer. Oncotarget 8: 48972-48982, 2017.
9. Croce CM: Causes and consequences of microRNA dysregulation in cancer. Nat Rev Genet 10: 704-714, 2009.
10. Calin GA and Croce CM: MicroRNA signatures in human cancers. Nat Rev Cancer 6: 857-866, 2006.
11. Li XY, Luo QF, Wei CK, Li DF, Li J and Fang L: MiRNA-107 inhibits proliferation and migration by targeting CDK8 in breast cancer. Int J Clin Exp Med 7: 32-40, 2014.
12. Dong X, Sui C, Huang K, Wang L, Hu D, Xiong T, Wang R and Zhang H: MicroRNA-223-3p suppresses leukemia inhibitory factor expression and pinopodes formation during embryo implantation in mice. Am J Transl Res 8: 1155-1163, 2016.
13. Zhou W, Pal AS, Hsu AY, Gurol T, Zhu X, Wirbisky-Hershberger SE, Freeman JL, Kasinski AL and Deng Q: MicroRNA-223 suppresses the canonical NF-κB pathway in basal keratinocytes to dampen neutrophilic inflammation. Cell Rep 22: 1810-1823, 2018.
14. Wong ML and Medrano JF: Real-time PCR for mRNA quantitation. Biotechniques 39: 75-85, 2005.
15. Baldwin AG, Tapia VS, Swanton T, White CS, Beswick JA, Brough D and Freeman S: Design, synthesis and evaluation of novel oxazaborine inhibitors of the NLRP3 inflammasome. ChemMedChem 13: 312-320, 2018.
16. Johnson JL, Ramadass M, Haimovich A, McGeough MD, Zhang J, Hoffman HM and Catz SD: Increased neutrophil secretion induced by NLRP3 mutation links the inflammasome to azurophilic granule exocytosis. Front Cell Infect Microbiol 7: 507, 2017.
17. Shi X, Qiu S, Zhuang W, Yuan N, Wang C, Zhang S, Sun T, Guo W, Gao F, Yang S and Qiao Y: NLRP3-inflammasomes are triggered by age-related hearing loss in the inner ear of mice. Am J Transl Res 9: 5611-5618, 2017.
18. Ismael S, Nasoohi S and Ishrat T: MCC950, the selective inhibitor of nucleotide oligomerization domain-like receptor protein-3 inflammasome, protects mice against traumatic brain injury. J Neurotrauma 35: 1294-1303, 2018.
19. Wu X, Dong L, Lin X and Li J: Relevance of the NLRP3 inflammasome in the pathogenesis of chronic liver disease. Front Immunol 8: 1728, 2017.
20. Zhao Y, Guo Q, Zhao K, Zhou Y, Li W, Pan C, Qiang L, Li Z and Lu N: Small molecule GL-V9 protects against colitis-associated colorectal cancer by limiting NLRP3 inflammasome through autophagy. Oncoimmunology 7: e1375640, 2017.
21. Hu Q, Zhao F, Guo F, Wang C and Fu Z: Polymeric nanoparticles induce NLRP3 inflammasome activation and promote breast cancer metastasis. Micromol Biosci 17, 2017.
22. Haque I, Ghosh A, Acup S, Banerjee S, Dhar K, Ray A, Sarkar S, Kambhampati S and Banerjee SK: Leptin-induced ER-α-positive breast cancer cell viability and migration is mediated by suppressing CCN5-signaling via activating JAK/AKT/STAT-pathway. BMC Cancer 18: 99, 2018.
23. Knutson TP, Daniel AR, Fan D, Silverstein KA, Covington KR, Fuqua SA and Lange CA: Phosphorylated and sumoylation-deficient progesterone receptors drive proliferative gene signatures during breast cancer progression. Breast Cancer Res 14: R95, 2012.
24. Okarvi SM and Aljammaz I: Preparation and in vitro and in vivo characterization of the tumor-specific antigen-derived peptide as a potential candidate for targeting human epidermal growth factor receptor 2-positive breast carcinomas. Anticancer Res 38: 2823-2830, 2018.
25. Salkho NM, Paul V, Kawak P, Vitor RF, Martins AM, Al Sayah M and Husseini GA: Ultrasonically controlled estrone-modified liposomes for estrogen-positive breast cancer therapy. Artif Cells Nanomed Biotechnol 12: 1-11, 2018.
26. Yang F, Xu Y, Liu C, Ma C, Zou S, Xu X, Jia J and Liu Z: NF-κB/miR-223-3p/ARID1A axis is involved in *Helicobacter pylori* CagA-induced gastric carcinogenesis and progression. Cell Death Dis 9: 12, 2018.
27. Hornung V and Latz E: Intracellular DNA recognition. Nat Rev Immunol 10: 123-130, 2010.
28. Quan JH, Huang R, Wang Z, Huang S, Choi IW, Zhou Y, Lee YH and Chu JQ: P2X7 receptor mediates NLRP3-dependent IL-1β secretion and parasite proliferation in Toxoplasma gondii-infected human small intestinal epithelial cells. Parasites Vectors 11: 1, 2018.
29. Pachathundikandi SK and Backert S: *Helicobacter pylori* controls NLRP3 expression by regulating hsa-miR-223-3p and IL-10 in cultured and primary human immune cells. Innate Immun 24: 11-23, 2018.
30. Daley D, Mani VR, Mohan N, Akkad N, Pandian GSDB, Savadkar S, Lee KB, Torres-Hernandez A, Aykut B, Diskin B, *et al*: NLRP3 signaling drives macrophage-induced adaptive immune suppression in pancreatic carcinoma. J Exp Med 6: 1711-1724, 2017.
31. van der Heijden T, Kritikou E, Venema W, van Duijn J, van Santbrink PJ, Slütter B, Foks AC, Bot I and Kuiper J: NLRP3 inflammasome inhibition by MCC950 reduces atherosclerotic lesion development in apolipoprotein E-deficient mice-brief report. Arterioscler Thromb Vasc Biol 37: 1457-1461, 2017.
32. Deswaerte V, Nguyen PM, West A, Browning AF, Yu L, Ruwanpura SM, Balic J, Livis T, Girard C, Preaudet A, *et al*: Inflammasome adaptor ASC suppresses apoptosis of gastric cancer cells by an IL18-mediated inflammation-independent mechanism. Cancer Res 78: 1293-1307, 2018.
33. Huang L, Li F, Deng P and Hu C: MicroRNA-223 promotes tumor progression in lung cancer A549 cells via activation of the NF-κB signaling pathway. Oncol Res 24: 405-413, 2016.
34. Guo J, Cao R, Yu X, Xiao Z and Chen Z: MicroRNA-223-3p inhibits human bladder cancer cell migration and invasion. Tumour Biol 39: 1010428317691678, 2017.
35. Fang G, Liu J, Wang Q, Huang X, Yang R, Pang Y and Yang M: MicroRNA-223-3p regulates ovarian cancer cell proliferation and invasion by targeting SOX11 expression. Int J Mol Sci 18: E1208, 2017.